Anisotropic material properties of fused deposition modeling ABS

Sung-Hoon Ahn
Michael Montero
Dan Odell
Shad Roundy and
Paul K. Wright

The authors

Sung-Hoon Ahn is at the Gyeongsang National University, Jinju, Korea 660-701

Michael Montero, **Dan Odell**, **Shad Roundy** and **Paul K. Wright** are at the University of California, Berkeley, California 94710, USA

Keywords

Rapid prototyping, Anisotropy, Fused deposition modeling

Abstract

Rapid Prototyping (RP) technologies provide the ability to fabricate initial prototypes from various model materials. Stratasys Fused Deposition Modeling (FDM) is a typical RP process that can fabricate prototypes out of ABS plastic. To predict the mechanical behavior of FDM parts, it is critical to understand the material properties of the raw FDM process material, and the effect that FDM build parameters have on anisotropic material properties. This paper characterizes the properties of ABS parts fabricated by the FDM 1650. Using a Design of Experiment (DOE) approach, the process parameters of FDM, such as raster orientation, air gap, bead width, color, and model temperature were examined. Tensile strengths and compressive strengths of directionally fabricated specimens were measured and compared with injection molded FDM ABS P400 material. For the FDM parts made with a 0.003 inch overlap between roads, the typical tensile strength ranged between 65 and 72 percent of the strength of injection molded ABS P400. The compressive strength ranged from 80 to 90 percent of the injection molded FDM ABS. Several build rules for designing FDM parts were formulated based on experimental results.

Electronic access

The research register for this journal is available at
http://www.emeraldinsight.com/researchregisters

The current issue and full text archive of this journal is available at
http://www.emeraldinsight.com/1355-2546.htm

Rapid Prototyping
Volume 8 · Number 4 · 2002 · pp. 248–257

DOI 10.1108/13552540210441166

1. Introduction

Recent advances in the fields of Computer Aided Design (CAD) and Rapid Prototyping (RP) have given designers the tools to rapidly generate an initial prototype from concept. There are currently several different RP technologies available, each with its own unique set of competencies and limitations. The Fused Deposition Modeling (FDM) process from Stratasys produces prototype parts out of ABS plastic. FDM deposits a molten filament of ABS in a criss-cross manner resulting in direction dependant, or anisotropic, material properties. This paper seeks to characterize some of the anisotropic properties of ABS parts produced by the FDM process.

The FDM process works as follows. First, a three dimensional solid model must be created. This can be accomplished in many of the commonly available CAD packages. The model is then exported to the FDM Quickslice™ software using the stereolithography (STL) format. This format tessellates the part into a set of triangles. The advantage of the STL format is that most CAD systems support it, and it simplifies the part geometry by reducing it to its most basic components. The disadvantage is that the part loses some resolution, because only triangles, and not true arcs, splines, etc., now represent the geometry (Wright, 2001). However, the errors introduced by these approximations are acceptable as long as they are less than the inaccuracy inherent in the manufacturing process.

Once the STL file has been exported to Quickslice™, it is horizontally sliced into many thin sections. These sections represent the two-dimensional contours that the FDM process will generate which, when stacked upon one another, will closely resemble the original three-dimensional part. This sectioning approach is common to all currently available RP processes. The software then uses this information to generate the process plan that controls the FDM machine's hardware (Figure 1).

In the physical process of fabrication, an ABS filament is fed through a heating element and becomes semi-molten. The filament is

Authors thank Seunghwa Kim, Hongkyung Lee, and Jaeil Lee for their assistance in the experiment. This work was partially supported by the Brain Korea 21 Project.

Figure 1 Fused deposition modeling process

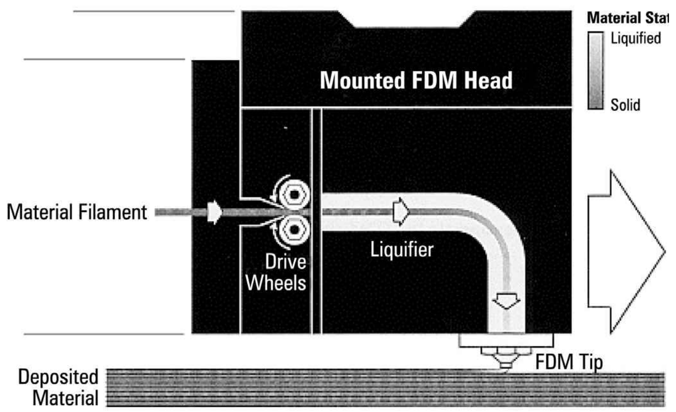

then fed through a nozzle and deposited onto the partially constructed part. Since the material is extruded in a semi-molten state, the newly deposited material fuses with adjacent material that has already been deposited. The head then moves around in the $X-Y$ plane and deposits material according to the part geometry. The platform holding the part then moves vertically in the Z plane to begin depositing a new layer on top of the previous one. After a period of time, usually several hours, the head will have deposited a full physical representation of the original CAD file.

The FDM machine possesses a second nozzle that extrudes support material and builds support for any structure that has an overhang angle of less than 45° from horizontal as a default. If the angle is less than 45°, more than one-half of one bead is overhanging the contour below it, and therefore is likely to fall.

The FDM process produces parts with unique characteristics. The machine deposits material in a directional way that results in parts with anisotropic behavior. Experiments were performed in which the effect of several process parameters on the mechanical behavior of FDM parts was examined.

2. Build parameter considerations

The first step in the experiment was to identify the process control parameters that were likely to affect the properties of FDM parts. The selected parameters are listed below.

Bead width: bead width is the thickness of the bead (or road) that the FDM nozzle deposits. It can vary from 0.3 mm (0.012 inch) to 1 mm (0.0396 inch) for the FDM 1650 machine.

Air gap: air gap is the space between the beads of FDM material. The default is zero, meaning that the beads just touch. It can be modified to leave a positive gap, which means that the beads of material do not touch. The positive gap results in a loosely packed structure that builds rapidly. The air gap value can also be modified to leave a negative gap, meaning that two beads partially occupy the same space. This results in a dense structure, which requires a longer build time.

Model build temperature: this parameter refers to the temperature of the heating element for the model material. It controls the viscosity of molten material that is extruded from the nozzle.

Raster orientation: refers to the direction of the beads of material (roads) relative to the loading of the part.

Color: FDM P400 ABS material is available in a variety of colors: white, blue, black, yellow, green, and red.

The following process parameters were neglected: envelope temperature (the temperature of the air around the part), slice height (which is similar to bead width in the vertical direction), and nozzle diameter (the width of the hole through which the material extrudes). These parameters seemed to be either duplicates of the selected parameters, or did not seem to have a relevant connection to the final material properties.

The envelope temperature appeared to have an insignificant effect on past parts prototyped with the FDM machine. Furthermore, the temperature in the envelope tends to fluctuate several degree Celsius during a build, making precise control of this variable difficult. The temperature may also vary in different locations in the build volume, increasing the control difficulty.

Slice height is the thickness of each layer measured in the vertical or Z direction. Varying the slice height would most likely have the same effect as varying the bead width of the ABS plastic. Since an individual bead of the material is homogenous, varying the geometry of the bead in one dimension should have the same effect as modifying it in the other dimension, causing a redundancy between this parameter and bead width. One factor that could affect this assumption is the fact that material is likely to have cooled more thoroughly between layers than between

Rapid Prototyping
Volume 8 · Number 4 · 2002 · 248–257

roads, potentially affecting the fusion of the plastic.

Similarly, the nozzle diameter was assumed to primarily affect the geometry of the bead. Since bead geometry was already being altered via road width (which is controlled by the flow rate of material through the nozzle), altering the nozzle diameter seemed to duplicate the testing. Effecting a nozzle change, which requires a physical transfer and re-calibration for every change, is much more time consuming than changing road width, which is easily modified in software.

3. Experiment setup

A trial run was performed in which a series of samples were built on the FDM machine by modifying the toolpaths in the Quickslice software (FDM, 1998). Views of parts with the toolpaths (or roads) from Quickslice are shown in Figure 2. An Instron® 8872 load frame with 25 kN load cell was used to load the test samples in tension.

The trial run samples were made according to the ASTM D638 (ASTM, 1997), type I standard. However, the geometry of these specimens revealed problems. As shown in Figures 3 and 4, the ASTM D638 shape added complications to the loading of the parts that caused them to fail prematurely.

These complications included large stress concentrations caused by the termination of the longitudinal roads used to approximate the large radii. These specimens failed prematurely by shearing at the stress concentrations, while the rest of the sample remained intact (Figure 3). As an attempt to remedy this, offset contours that followed the perimeter of the sample were used to relieve the stress concentrations. However, this approach caused stress-concentrating gaps in the center of the sample, as well as areas where the roads were no longer in pure tension, defeating the intent of the D638 standard. These samples tended to fail prematurely at these areas of multi-state stress (Figure 4).

In response to these complications, another specimen geometry, ASTM D3039 (ASTM, 1976) was adapted for the tensile test coupon. The specimen had size of 229 mm × 25.4 mm × 3.3 mm. The loading rate of the test was 2 mm/min. The load and strain data for each sample was collected as it was loaded.

Figure 2 Quickslice SML file showing samples with bead width, air gap, and raster orientation variation

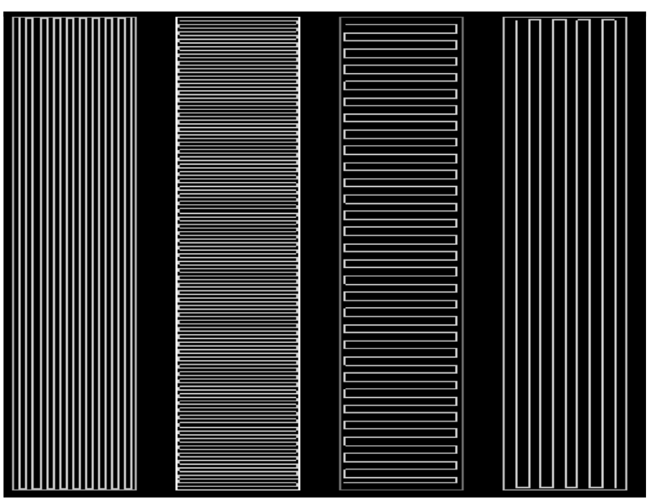

Figure 3 Premature shear failure of ASTM D638 standard test specimens with longitudinal roads

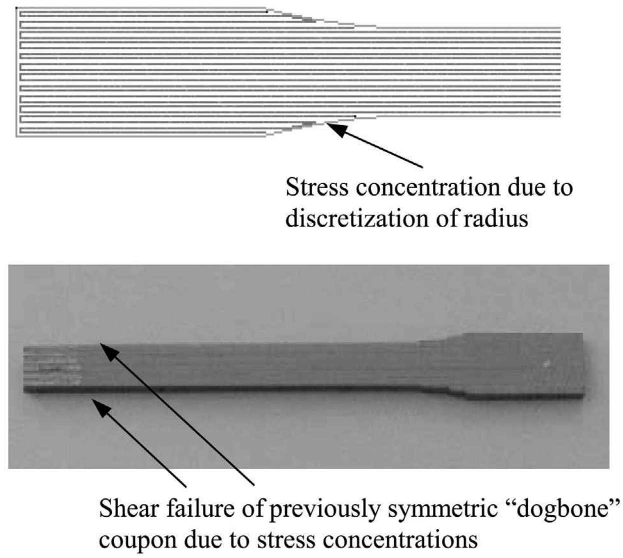

Figure 4 Premature shear failure of ASTM D638 standard test specimens with offset contours

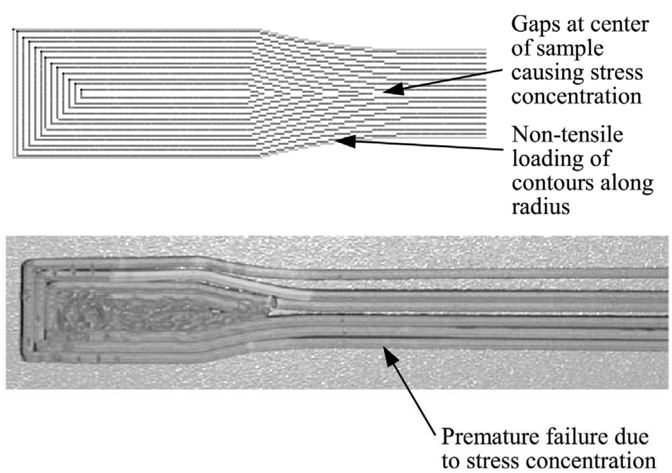

Rapid Prototyping
Volume 8 · Number 4 · 2002 · 248–257

4. Design of experiment

The goal of the experiment was to determine the effect of changing selected design and process variables on the tensile strength of the FDM test specimens. As mentioned earlier, the variables selected for this experiment were chosen from a larger set based on the experience and knowledge of the researchers. Figure 5 shows a more complete set of variables and the domain or classification under which each one falls.

The five variables selected came from three different classifications: unprocessed ABS material, FDM build specifications, and FDM environment. The five variables are air gap, bead width, model temperature, ABS color, and raster orientation. Among the five variables, one variable is qualitative (ABS color) whereas the remaining four are quantitative parameters. The next step in setting up the DOE was to determine the resolution for the experiment and the number of levels for each variable (Wu and Hamada, 2000 and Box *et al.*, 1978).

A linear relationship between the response (tensile strength) and the five experiment variables was expected (see Table I). For this reason, each parameter requires only two levels, one set high (+ 1), and one set low (− 1). In order to set the appropriate levels, preliminary tests were conducted for each variable to define its range. Each variable was varied independently, and the tensile strength was measured. The results of these preliminary tests provided the settings for the levels of each parameter.

All main effects and multi-factor interaction effects were multiplied by the defining relation to reveal the confounding terms within each effect estimate. Not only does the generator and defining relation help derive the effect estimates, but they also help in setting the appropriate test conditions or treatments for the design matrix. Since the generator is E = ABCD, the coded levels for parameter E, or column E will be defined by the product of coded units (+ 1 and − 1) of columns A, B, C, and D (See Figure 6a). With only 16 test conditions, it was decided to replicate each one in order to calculate an estimate of the standard error within the experiment. The final design contains a total of 32 test specimens, which is an advantage over a full factorial design (2^5) that contains the same number of runs but lacks the estimate of error. Figure 6b shows that variables A (air gap) and E (raster) had a significant effect on the tensile strength response. More details of the experimental design and analysis of the build parameters of FDM material can be found in the authors' earlier work (Montero *et al.*, 2001).

Figure 5 Fishbone diagram of potential factors influencing tensile strength

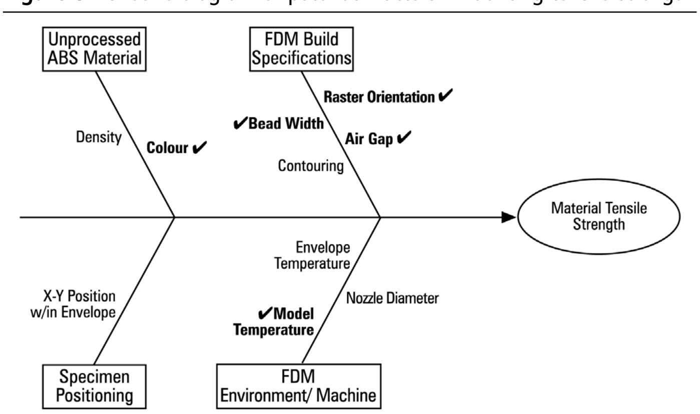

Table I Variable symbols and level settings

Variable	Symbol	Levels Low(−)	High(+)
Air gap (inch/mm)	A	0.0/0.0	−0.002/−0.0508
Road width (inch/mm)	B	0.02/0.508	0.0396/1.00
Model temperature (°C)	C	270	280
ABS color	D	Blue	White
Orientation of rasters	E	Transverse	Axial

5. Injection molded ABS

In order to measure the reference strength of the ABS P400 material, tensile and compression specimens were fabricated by injection molding. This process yields much more isotropic parts than the FDM process. The same material was used for specimens produced by both FDM and injection molding.

First, aluminum molds for tensile and compression specimens were milled on a three-axis CNC machine. The dimensions of the mold cavity for the tensile specimen were the same as those of the specimen described in the Experiment Setup section (229 mm × 25.4 mm × 3.3 mm). The shrinkage of the molded ABS was not considered because the reduced cross section would be normalized to the actual cross sectional area for strength values. The dimensions of the compression specimens were 25.4 mm (1 inch) in length and 12.7 mm (0.5 inch) in diameter according to ASTM D695 (ASTM, 1996).

Figure 6 Test matrix and plot of tensile strength (MPa) versus main effects (Montero *et al.*, 2001)

Run	A	B	C	D	E
1	−	−	−	−	+
2	+	−	−	−	−
3	−	+	−	−	−
4	+	+	−	−	+
5	−	−	+	−	−
6	+	−	+	−	+
7	−	+	+	−	+
8	+	+	+	−	−
9	−	−	−	+	−
10	+	−	−	+	+
11	−	+	−	+	+
12	+	+	−	+	−
13	−	−	+	+	+
14	+	−	+	+	−
15	−	+	+	+	−
16	+	+	+	+	+

(a)

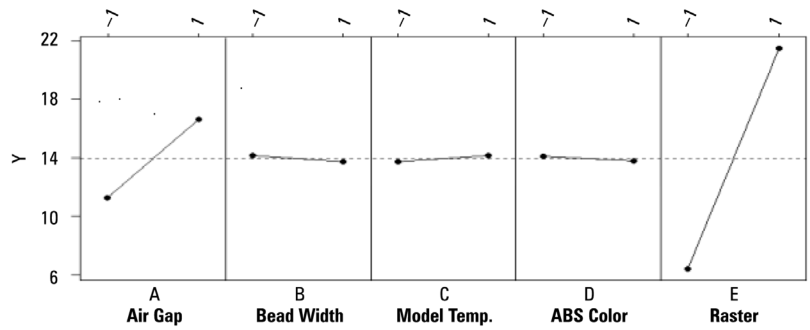

(b)

The injection molded samples were created by cutting strands of ABS P400 into 3–5 mm long pieces for use in the Morgan Press G-100T injection molding machine (Figure 7). The nozzle temperature of the injection press was 270°C, the mold preheat temperature was 120°C, the clamping force was 16,000 lbf (71 kN), and the injection pressure was 6,000 psi (41 MPa). These injection parameters for injection molding were the typical values applied for ABS plastic using this machine.

6. Results

Dozens of specimens were produced by FDM for comparison with the samples produced by injection molding. For each type of the specimen, three to five replications were fabricated and tested. The DOE showed that air gap and raster orientation were the only significant effects. Therefore, the effect of these two variables on the tensile strength of specimens was considered more closely.

6.1 Tensile tests

Each FDM specimen consisted of 12 layers with various raster orientations. For example, the axial specimen had 12 layers in the zero (loading) direction $[0^\circ]_{12}$, and the criss-cross specimen had six repetitions of a 45° layer followed by a −45° layer $[45^\circ/-45^\circ]_6$.

Default FDM parts were made with a criss-cross raster in which the orientation of the beads alternates from + 45° to −45° from layer to layer. Some criss-cross raster

Figure 7 Process of fabricating tensile and compression specimens by injection molding of chopped FDM material

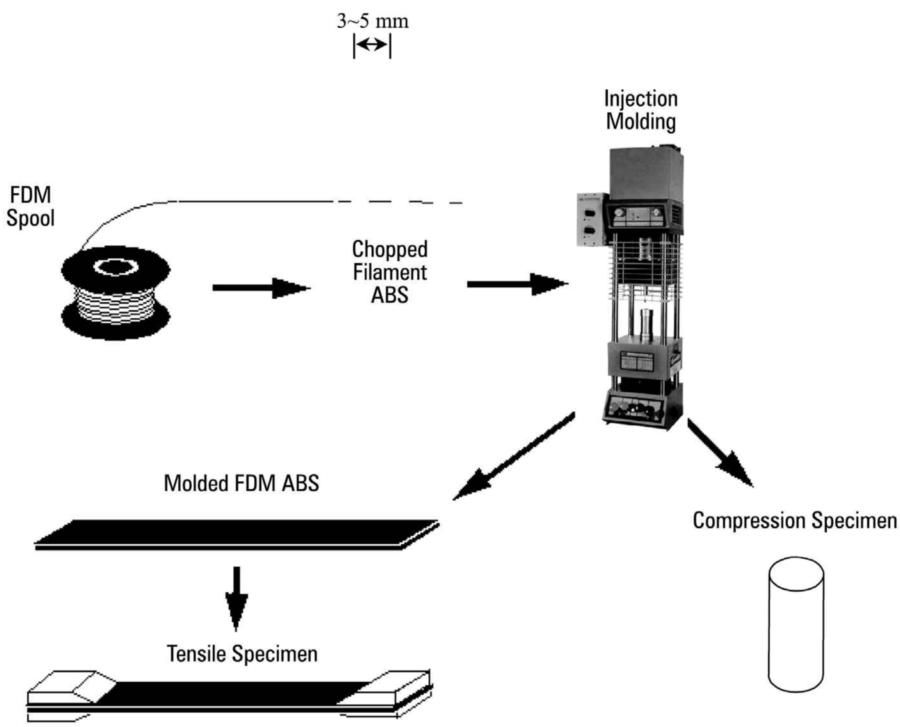

specimens were built and tested in addition to the main factorial experiment.

Figure 8 shows the resulting tensile strength values for the specimens with zero air gap. The injection molded ABS P400 failed at 26 MPa, and the four FDM specimens failed between 10 and 73 percent of the injection molded P400's strength, depending on raster orientation.

Figure 9 shows the effect of a negative (−0.003) air gap, which makes the specimen more dense and strong. Although the strength of the axial specimens was not increased much with a negative air gap, other FDM specimens exhibited a large increase in tensile strength. The [45°/−45°] raster orientation is of particular interest as the Quickslice software defaults to this raster. This orientation could be looked at as a [0°/90°] orientation if the part were rotated 45°. For these two general cases, the strength ranged between 65 and 72 percent of the injection molded P400.

The failure modes of these specimens are shown in Figure 10. All specimens failed in transverse direction except the criss-cross specimen, which failed along the 45° line. The failure modes for specimens with zero air gap were identical to those with −0.003 air gap. The relationship between failure loads and

Figure 8 Tensile strength of specimens with various raster (zero air gap) compared with injection molded ABS P400

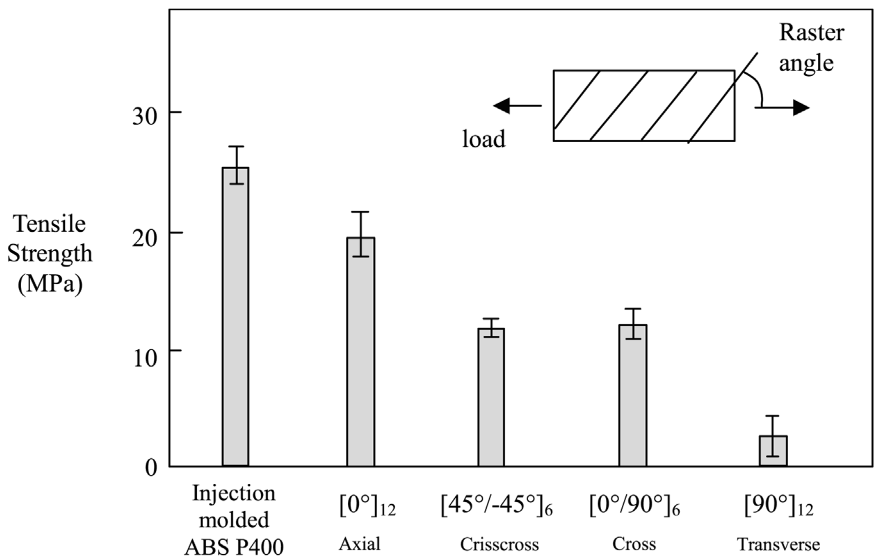

Figure 9 Tensile strength specimens with various raster (−0.003 inch air gap) compared with injection molded ABS P400

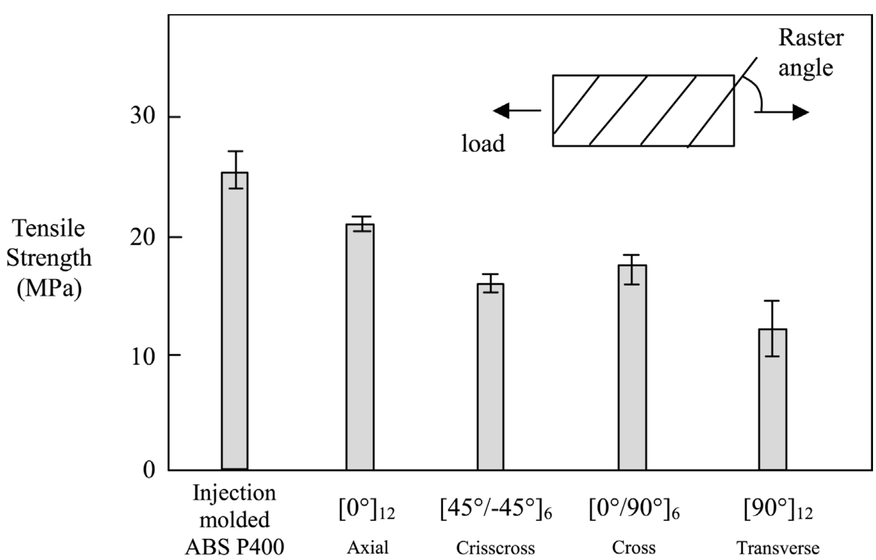

Figure 10 Failure modes of the specimens with various raster orientations (-0.003 air gap) compared with injection molded ABS P400

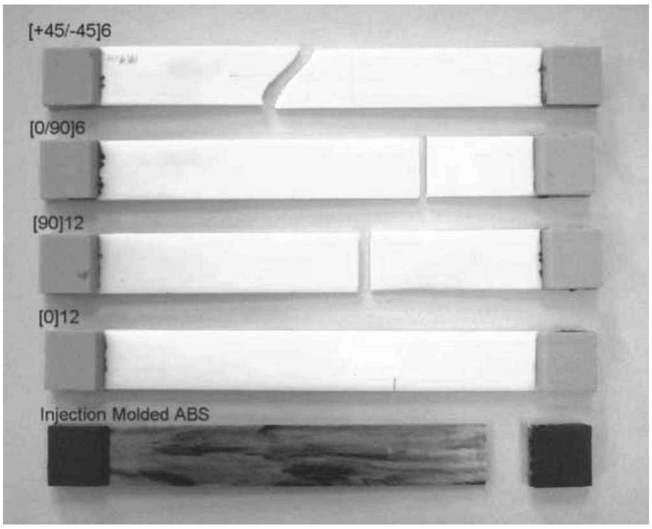

failure modes required microscopic observations.

Figure 11 shows magnified views of the fractured surfaces of the specimens. The Axial ($[0^{\circ}]_{12}$) specimens (Figure 11a) showed tensile failure of individual fibers resulting in the highest tensile strength among the FDM specimens (Figure 9). However, this strength was lower than that of the injection molded ABS partially because the gaps between fibers reduced the effective cross sectional area. The Transverse ($[90^{\circ}]_{12}$) specimens resulted in the lowest tensile strength because the tensile loads were taken only by the bonding between fibers, and not the fibers themselves. The Cross specimen ($[0^{\circ}/90^{\circ}]_{6}$) consisted of a layer of fibers oriented in the 0° direction, followed by a layer in the 90° direction. The resulting failure load for this pattern, as might be expected, fell between the $[0^{\circ}]_{12}$ and $[90^{\circ}]_{12}$ specimens. The Criss-cross ($[45^{\circ}/-45^{\circ}]_{6}$) specimen showed shear failure along the 45° line in the macroscopic view (Figure 10), but the microscopic view revealed the repeated failures of individual fibers by shearing and tension (Figure 11b). Note that the oval shape of the fibers is determined by the Quickslice software settings for road width and slice height.

6.2 Compression tests

For the compression tests, build direction was the only examined parameter. Because the complexity of test increases with more parameters, other possible control parameters such as raster angle and air gap were not considered in this experiment. "Axial" (horizontal) and "Transverse" (vertical) directions were defined as shown in Figure 12. With a fixed raster angle of $[45^{\circ}/-45^{\circ}]$ and zero air gap, the effect of build direction on compression strength could be measured. This effect would be difficult to measure in a tension specimen because the slender and long geometries involved would result in a high probability of buckling.

Figure 11 Scanning electron microscope (SEM) pictures of the fracture surfaces of (a) a $[0^{\circ}]_{12}$ specimen and (b) a $[45^{\circ}/-45^{\circ}]_{6}$ specimen both with -0.003 inch air gap

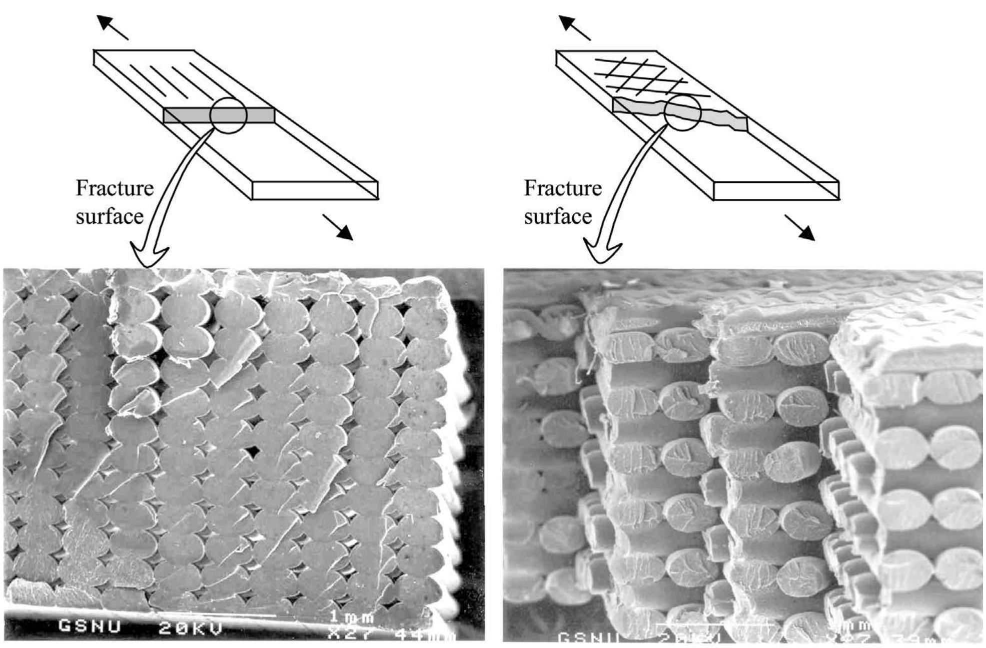

(a) $[0^{\circ}]_{12}$ specimen
(b) $[45^{\circ}/-45^{\circ}]_{6}$ specimen

Figure 12 Compression specimens with two different build directions

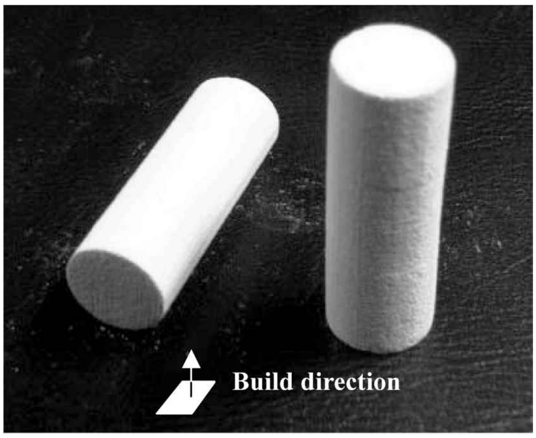

Figure 13 shows higher compressive strengths compared to the tensile strengths shown in Figure 8. Higher compressive strengths are often observed in polymers, and for bulk ABS materials. For example, tensile strengths of typical bulk ABS range from 32 to 45 MPa while their compressive strengths range from 65 to 90 MPa (ASM, 1988). The Transverse specimen had 15 percent lower compressive strength than the axial specimen. In general, the compressive strengths of FDM specimens ranged from 80 to 90 percent of those for injection molded ABS

7. Build rules

Build rules have been formulated based on the results of the experiments. These guidelines are intended to aid designers in improving the strength and accuracy of their parts made on the FDM machine. These rules are listed with a few illustrative examples of how a rule might apply to a given situation.

Rule 1: Build parts such that tensile loads will be carried axially along the fibers

Figure 14 shows a boss along with two cross sections. Two possible orientations for the roads are shown. In the first cross section, the roads follow the contour of the boss. If a screw were threaded into the boss, the maximum stress (the hoop stress) would be carried axially by the fibers going around the contour of the boss. The second cross section is the default orientation that the FDM software would choose. The maximum stress would be carried across the bonds in this case, resulting in a higher probability of failure.

Figure 15 shows a cantilever snap fit. Again two different possible build orientations are shown. In the first cross section, the maximum stress (a bending stress in this case) occurs along the roads, while in the second, the maximum stress is carried across the roads. Of course, the cantilever built in the first orientation will be significantly stronger.

Rule 2: Be aware that stress concentrations occur at radiused corners. This is because the FDM roads exhibit discontinuities at such transitions

Figure 16 shows a standard ASTM D3039 tensile specimen that was not used for these tests for reasons already mentioned.

Figure 13 Compressive strength of specimens with different build direction compared with injection molded ABS P400. Specimens were built with raster angle of [45°/−45°] and 0 air gap

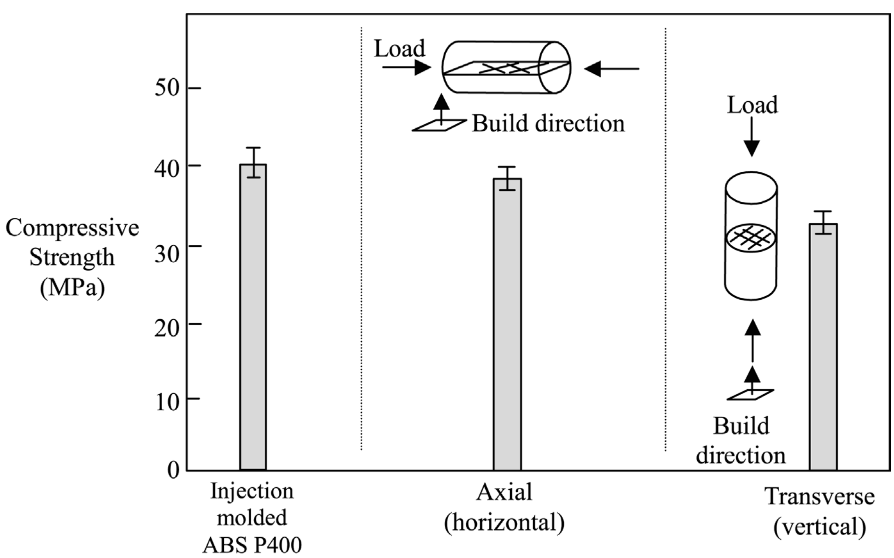

Figure 14 Two different road orientations for boss design

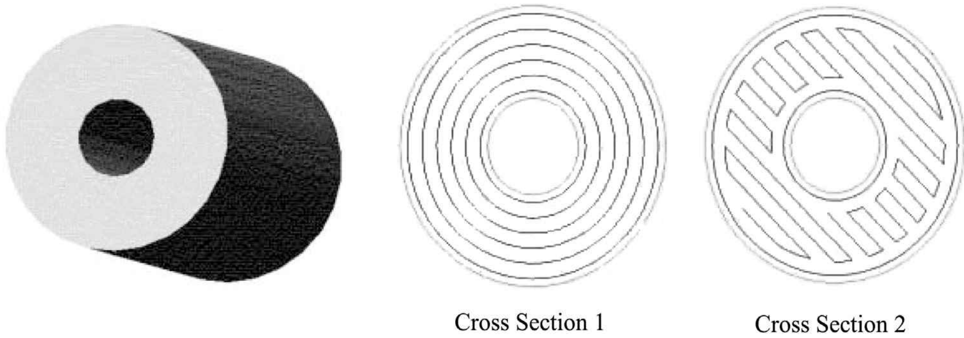

Figure 15 Two different road orientations for snap-fit design

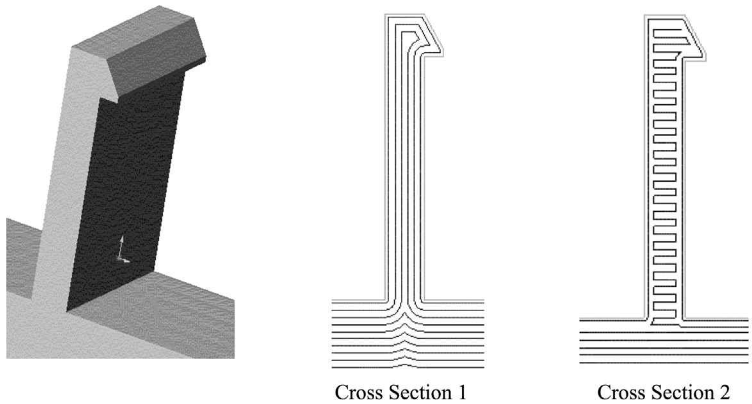

Notice that although the radius is large, there are extreme stress concentrations in the first cross section where the vertical roads terminate. All the parts that were built and tested in this configuration fractured on the radius where these stress concentrations occur. Cross section 2 shows a better alternative. However, although the stress concentrations along the surface of the radius have been removed, stress concentrations in the center of the part have been created. An additional problem is that the roads are no longer loaded in pure tension through the radiused part of the specimen. In general, when a radiused area will be carrying a load, it is best to build that radius with contours to alleviate the extreme stress concentrations that can occur due to rasterization.

Rule 3: Use a negative air gap to increase both strength and stiffness

If strength is of primary concern, a negative air gap can be used to create a stronger part. However, an air gap less than −0.003 inches

Figure 16 Two different road orientations for ASTM D3039 design

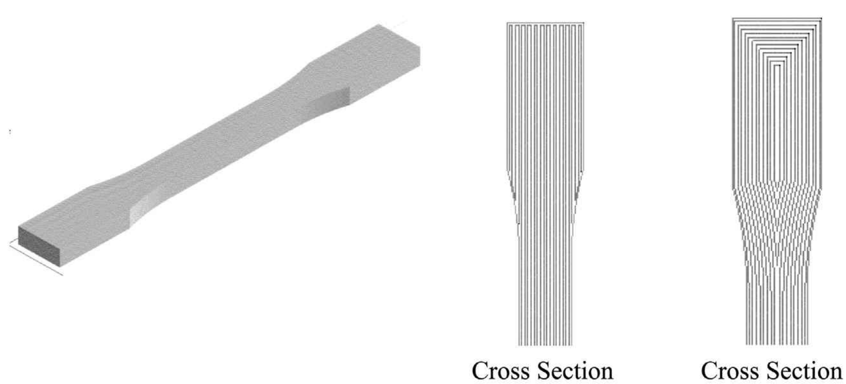

Rapid Prototyping
Volume 8 · Number 4 · 2002 · 248–257

should not be used. It was found that parts with an air gap smaller than this simply did not build well due to excess material build up on the nozzle and the part itself. It should be noted that for relatively thick parts, a negative air gap can degrade surface quality and dimensional tolerances.

Rule 4: Consider the following issues on bead width

- Small bead width increases build time.
- Small bead width improves surface quality.
- Wall thickness of the part should be an integer multiple of the bead width to avoid gaps.

Rule 5: Consider the effect of build orientation on part accuracy

- Two-dimension slices closely reproduce geometry.
- Three-dimension layer stacking creates linear approximations.

Rule 6: Be aware that tensile loaded area tends to fail easier than compression loaded area

Maximum compression strengths of FDM specimens are approximately double of tensile strengths.

8. Conclusions

From the Design of Experiment for FDM ABS (P400), it was found that the air gap and raster orientation affect the tensile strength of an FDM part greatly. Bead width, model temperature, and color have little effect. The measured material properties showed that parts made by FDM have anisotropic characteristics. Measured tensile strengths of the typical Criss-cross raster [$45^\circ/-45^\circ$] and Cross raster [$0^\circ/90^\circ$] with -0.003 air gap were between 65 and 72 percent of the measured strength of injection molded FDM ABS. The compressive strength of FDM material was higher than the tensile strength and was not affected much by build direction. Because of the anisotropic behavior of the parts made by the FDM process, the strength of a local area in the part depends on the raster direction.

Following build rules were obtained from this study.

(1) Build parts such that tensile loads will be carried axially along the fibers.
(2) Be aware that stress concentrations occur at radiused corners. This is because the FDM roads exhibit discontinuities at such transitions.
(3) Use a negative air gap to increase both strength and stiffness.
(4) Consider the following issues on bead width.
    - Small bead width increases build time.
    - Small bead width increases surface quality.
    - Wall thickness of the part should be an integer multiple of the bead width.
(5) Consider the effect of build orientation on part accuracy.
(6) Be aware that tensile loaded area tends to fail easier than compression loaded area.

By applying these build rules, the strength and quality of FDM parts can be improved.

References

ASM (1988), *Engineered Materials Handbook*, Vol. 2, Engineering Plastic, ASM International.

ASTM (1976), ASTM D3039-76, Test Method for Tensile Properties of Polymer Matrix Composite Materials, ASTM.

ASTM (1996), ASTM D695-96, Test Method for Compressive Properties of Rigid Plastics, ASTM.

ASTM (1997), ASTM D638-97, Test Method for Tensile Properties of Plastics, ASTM.

Box, G., Hunter, W. and Hunter, J. (1978), *Statistics for Experimenters: An Introduction to Design, Data Analysis, and Model Building*, John Wiley & Sons, Inc.

FDM (1998), FDM® (System Documentation, Stratasys, Inc.

Montero, M., Odell, D., Roundy, S., Ahn, S.H. and Wright, P.K. (2001), "Material Characterization of Fused Deposition Modeling (FDM) Process," Rapid Prototyping and Manufacturing Conference, Society of Manufacturing Engineers, May 15-17, Cincinnati, OH, 2001.

Wright, P.K. (2001), *21st Century Manufacturing*, Prentice Hall.

Wu, J. and Hamada, M. (2000), *Experiments: Planning, Analysis, and Parameter Design Optimization*, John Wiley & Sons, Inc.